Inorganic Chemistry

Article

pubs.acs.org/IC

Engineered Recognition of Tetravalent Zirconium and Thorium by Chelator−Protein Systems: Toward Flexible Radiotherapy and Imaging Platforms

Ilya Captain,[†] Gauthier J.-P. Deblonde,[†] Peter B. Rupert,[‡] Dahlia D. An,[†] Marie-Claire Illy,[†] Emeline Rostan,[†] Corie Y. Ralston,[§] Roland K. Strong,*[,‡] and Rebecca J. Abergel*[,†]

[†]Chemical Sciences Division, Lawrence Berkeley National Laboratory, Berkeley, California 94720, United States

[‡]Division of Basic Sciences, Fred Hutchinson Cancer Research Center, Seattle, Washington 98109, United States

[§]Berkeley Center for Structural Biology, Lawrence Berkeley National Laboratory, Berkeley, California 94720, United States

Supporting Information

ABSTRACT: Targeted α therapy holds tremendous potential as a cancer treatment: it offers the possibility of delivering a highly cytotoxic dose to targeted cells while minimizing damage to surrounding healthy tissue. The metallic α-generating radioisotopes ^{225}Ac and ^{227}Th are promising radionuclides for therapeutic use, provided adequate chelation and targeting. Here we demonstrate a new chelating platform composed of a multidentate high-affinity oxygen-donating ligand 3,4,3-LI(CAM) bound to the mammalian protein siderocalin. Respective stability constants log β_{110} = 29.65 ± 0.65, 57.26 ± 0.20, and 47.71 ± 0.08, determined for the Eu^{III} (a lanthanide surrogate for Ac^{III}), Zr^{IV}, and Th^{IV} complexes of 3,4,3-LI(CAM) through spectrophotometric titrations, reveal this ligand to be one of the most powerful chelators for both trivalent and tetravalent metal ions at physiological pH. The resulting metal−ligand complexes are also recognized with extremely high affinity by the siderophore-binding protein siderocalin, with dissociation constants below 40 nM and tight electrostatic interactions, as evidenced by X-ray structures of the protein:ligand:metal adducts with Zr^{IV} and Th^{IV}. Finally, differences in biodistribution profiles between free and siderocalin-bound $^{238}Pu^{IV}$-3,4,3-LI(CAM) complexes confirm *in vivo* stability of the protein construct. The siderocalin:3,4,3-LI(CAM) assembly can therefore serve as a "lock" to consolidate binding to the therapeutic ^{225}Ac and ^{227}Th isotopes or to the positron emission tomography emitter ^{89}Zr, independent of metal valence state.

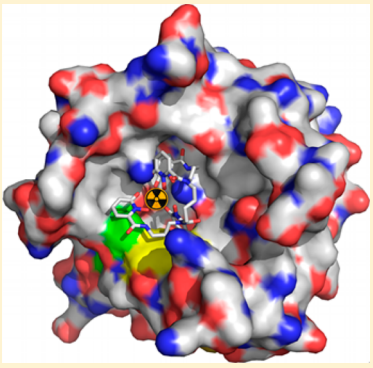

INTRODUCTION

Targeted α therapy (TAT), or radioimmunotherapy that uses α-particle emitting nuclides, is a promising treatment strategy for small metastatic tumors and other localized diseases. Owing to α-particles' short path length, much of the decay energy may be deposited into target areas while mitigating damage to surrounding tissue.[1] A number of radionuclides that emit single α particles, including ^{211}At ($t_{1/2}$ = 7.2 h), ^{213}Bi ($t_{1/2}$ = 0.8 h), and ^{212}Bi ($t_{1/2}$ = 1.0 h), are currently under investigation.[2] A growing subset of the field includes *in vivo* α-generator radionuclides ^{225}Ac ($t_{1/2}$ = 10.0 d), ^{223}Ra ($t_{1/2}$ = 11.4 d), and ^{227}Th ($t_{1/2}$ = 18.7 d), isotopes that emit multiple α particles in their decay chains and dramatically increase the potential delivered dose.[3−6] This principle was recently exploited in the development of Alpharadin, $^{223}RaCl_2$, a drug for bone metastases.[7] While Alpharadin relies on the natural propensity of ^{223}Ra for bone, other specifically targeted α-radiation delivery strategies use constructs formed with chelating agents to complex metallic α-emitters and biological targeting vectors.[2] Though sound in theory, these designs have been slow to appear in the clinic, with only scarce examples of promising α-generator immunoconjugates, such as the lintuzumab conjugate ^{225}Ac-HuM195[8] and the sialic-acid receptor CD33 conjugate ^{227}Th-CD33-TTC[9] for myeloid leukemia treatment, or ^{227}Th-DOTA-trastuzumab for treating HER-2 positive breast and ovarian cancer.[10] Reasons for this slow development are largely economical and related to costs associated with radionuclide production, clinical material production, as well as preclinical and clinical studies. Nevertheless, a better understanding of radiometal chelation and biodistribution is also direly needed to advance this field and to provide new chelating platforms that may be tailored on the basis of indication and isotope selection.

The ^{225}Ac and ^{227}Th radioisotopes are members of the actinide (An) series of elements. They display high coordination numbers and are best chelated by high-denticity ligands that contain hard donor atoms, such as the multidentate hydroxypyridinone-based (HOPO) compounds, our workhorse ligands for *in vivo* actinide decorporation.[11] The ligand 3,4,3-LI(1,2-HOPO) is an octadentate, tetraprotic compound composed of 4 bidentate 1,2-HOPO metal-binding units attached onto a spermine ("3,4,3-LI") scaffold (Figure 1). 3,4,3-LI(1,2-HOPO) was recently modified to enable monoclonal antibody attachment and form a bioconjugate chelator

Received: August 23, 2016

DOI: 10.1021/acs.inorgchem.6b02041
Inorg. Chem. XXXX, XXX, XXX−XXX

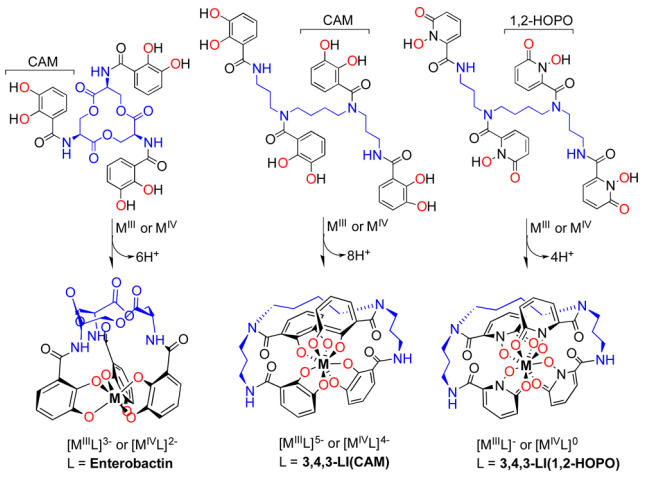

Figure 1. Complexation of M^{III} and M^{IV} by the hexadentate siderophore enterobactin or the octadentate synthetic analogues 3,4,3-LI(CAM) or 3,4,3-LI(1,2-HOPO), when deprotonated. Polyamine scaffolds and metal-binding oxygen atoms are highlighted in blue and red, respectively.

that displayed high *in vivo* stability when bound to ^{89}Zr, as imaged by positron emission tomography (PET).[12,13] Similarly, an octadentate Me-3,2-HOPO bioconjugate chelator built on a slightly different symmetrical polyamine scaffold was recently prepared for the complexation of ^{227}Th, and it displayed fast radiolabeling kinetics.[14] Although successful, such modifications necessitate extensive synthetic procedures with low overall yields,[12,14] which prompted us to investigate alternate routes to link therapeutic and imaging radionuclides to targeting moieties.

The mammalian 24 kDa glycoprotein siderocalin (Scn) is a member of the lipocalin protein superfamily. Scn is known to complement the innate immune system by binding specific bacterial siderophores and their ferric complexes, a mechanism that counters the iron acquisition pathway of invading microorganisms.[19] Our recent work revealed that Scn binds lanthanide (Ln) and An ions precomplexed with a suitable ligand in solution with very high affinity, through strong electrostatic interactions.[15] Although $[Fe^{III}(Ent)]^{3-}$, the ferric complex of the hexadentate catecholate siderophore enterobactin (Ent) is Scn's native ligand,[16] the protein's sterically hindered binding pocket was shown to bind Ln and An complexes of Ent (Figure 1).[15] More surprisingly, the protein also accommodates the much stronger Ln and An complexes formed with the octadentate synthetic analogue 3,4,3-LI(1,2-HOPO).[15] Building on this work, one can envision using the Scn−ligand−metal system as a radionuclide binder for TAT as well as a reporter ligand for concurrent diagnostics. The advantage of using a protein-mediated binding system is 2-fold: potentially tighter binding to nuclides of interest and easier attachment to targeting moieties by eliminating the need for post protein expression bioconjugate chemistry. The aforementioned $^{225}Ac^{III}$ and $^{227}Th^{IV}$ show promise in radioimmunotherapy, while $^{89}Zr^{IV}$ is useful as a PET tracer; all of these metals may be captured by the Scn−ligand system with some optimization. Upon single deprotonation of each of the 1,2-HOPO units (Figure 1), the overall negative 3,4,3-LI(1,2-HOPO) complexes of Ln^{III} and An^{III} are tightly bound by Scn, but the formally neutral 3,4,3-LI(1,2-HOPO) complexes of 4+ metals interact weakly.[15] The difference in binding originates from insufficient electrostatic interaction between the metal−ligand complex and Scn. In order to restore complex binding by Scn, we must use a ligand of high denticity that captures both 3+ and 4+ metals, forms overall negatively charged complexes, and does not cause steric clashes in Scn's tight binding pocket. This work aims to address the inability of the Scn-3,4,3-LI(1,2-HOPO) system to bind 4+ ions by exploring more suitable ligands that can complex both 3+ and 4+ metal ions.

METHODS

Caution! *^{232}Th, ^{238}Pu, ^{242}Pu, ^{243}Am, and ^{248}Cm are hazardous radionuclides with high specific activities that should only be manipulated in specifically designated facilities in accordance with appropriate safety controls.*

General Considerations. Chemicals were obtained from commercial suppliers and were used as received. The $LnCl_3 \cdot nH_2O$ lanthanide salts utilized were of the highest purity available (>99.9%). Stock solutions of $^{232}Th^{IV}$ and Zr^{IV} were prepared from $^{232}ThCl_4 \cdot 8H_2O$ (Baker & Adamson, ACS grade) and $ZrCl_4$ (Sigma-Aldrich, 99.99%), respectively. A stock of $^{238}Pu^{IV}$ was purchased as $^{238}Pu(NO_3)_4$ in 4 M HNO_3 from Eckert & Ziegler (lot 118521). ^{242}Pu was received from Oak Ridge National Laboratory as PuO_2 (lot Pu-242-327 A, 99.93 wt % of metal ^{242}Pu), and a stock solution of $^{242}Pu^{IV}$ was prepared as described previously.[17] The ^{242}Pu isotope was used for *in vitro* binding experiments whereas ^{238}Pu was used in biodistribution studies. Aliquots of acidified stocks of carrier-free ^{243}Am and ^{248}Cm (95.78% ^{248}Cm, 4.12% ^{246}Cm, 0.06% ^{245}Cm, 0.02% $^{244}Cm/^{247}Cm$ isotopic distribution by atom percentage) from Lawrence Berkeley National Laboratory were used. All solutions were prepared using deionized water purified by a Millipore Milli-Q reverse osmosis cartridge system, and the pH was adjusted with concentrated HCl, H_2SO_4, KOH, or NaOH when needed. Measurements were conducted at room temperature using standard instrumentation unless otherwise noted (see Supporting Information for details).

Metal, Ligand, and Protein Working Solutions. The trivalent lanthanide Ln^{III} working stock solutions were prepared in standardized 0.1 M HCl. A Zr^{IV} stock solution was prepared by dissolving $ZrCl_4$ in 3.0 M H_2SO_4, to prevent hydrolysis. The metal salt $ZrCl_4$ was handled and stored in a glovebox kept under inert atmosphere. The Zr^{IV} stock solution was standardized against EDTA, with xylene orange as the indicator.[18] A Th^{IV} stock solution was prepared in 0.1 M H_2SO_4. Stock solutions (4 mM) of Ent and 3,4,3-LI(CAM) were prepared by direct dissolution of a weighed portion of ligand in DMSO, and aliquots were removed prior to each set of experiments. Recombinant human Scn was prepared as previously described.[19]

Incremental Spectrophotometric Titrations. This method was used to determine the protonation constants of 3,4,3-LI(CAM) as well as the stability constants of its complexes formed with Eu^{III}, Zr^{IV}, and $^{232}Th^{IV}$. The experimental titration setup is similar to previously described systems, and details are provided as Supporting Information.[20] For the 3,4,3-LI(CAM) protonation (and Eu^{III}-3,4,3-LI(CAM) complexes), titrations were performed with an initial concentration of 50 μM of 3,4,3-LI(CAM) (and 50 μM of Eu^{III}) resulting in absorbance values between 0 and 1.0 throughout the titration. For the Zr^{IV} and Th^{IV} complexes, titrations were performed similarly but in the presence of DTPA to avoid the formation of metal hydroxides at low pH, before the uptake by 3,4,3-LI(CAM).

DOI: 10.1021/acs.inorgchem.6b02041
Inorg. Chem. XXXX, XXX, XXX−XXX

Protein-Binding Assay and Crystallography. Scn binding of metal−ligand complexes was measured by fluorescence quenching, as described previously[15,21] and detailed in the Supporting Information. Diffraction-quality crystals were grown by vapor diffusion from drops containing the ternary metal−chelator−protein complex according to standard methods (Supporting Information). Diffraction data were collected on beamline 5.0.2 at the Advanced Light Source (ALS, Berkeley, CA) and processed as detailed in Supporting Information. Crystallographic statistics are reported in Supporting Information Table S1. Final models have been deposited in the PDB.[22]

***In Vivo* Biodistribution Assay.** All procedures and protocols used in the presented *in vivo* studies were reviewed and approved by the Institutional Animal Care and Use Committee at Lawrence Berkeley National Laboratory and performed in AAALAC accredited facilities. The animals used were adult female CD-1 mice (180 ± 7 days old, 40.8 ± 5.8 g). Solutions of ^{238}Pu complexed by 3,4,3-LI(CAM) and Scn:3,4,3-LI(CAM) were prepared *in situ* at molar ratios protein:ligand:^{238}Pu of 0:100:1 and 100:100:1, respectively, by mixing and incubating the appropriate quantities of $^{238}Pu(NO_3)_4$, ligand, and protein in phosphate-buffered saline (PBS) to reach a ^{238}Pu concentration of 12 ng L^{-1}. Protein solutions were washed thrice with PBS using 10 kDa molecular weight cutoff membrane-based centrifugal filters, and all solutions were filter-sterilized (0.22 μm) prior to injection. Under isoflurane anesthesia, groups of three normally fed mice were injected intravenously with 0.2 mL of a complex solution (370 Bq per mouse). After injection of the ^{238}Pu tracer, mice were weighed, identified, and housed in groups of three in plastic stock cages lined with a 0.5 cm layer of highly absorbent low-ash pelleted cellulose bedding (Alpha-dri) for separation of urine and feces. Mice were given water and food *ad libitum* and euthanized at 4, 24, or 48 h after tracer injection. All experiments using ^{238}Pu tracers were managed as metabolic balance studies, in which tissues and excreta were analyzed for ^{238}Pu by liquid scintillation counting on a Perkin-Elmer Packard Tri-Carb model B4430. The methods of sample collection, preparation, radioactivity measurements, and data reduction have been published previously.[23−25] Those methods provide quantitative measurements of radioactivity in biological samples; material recoveries averaged about 99% of the amount injected in these experiments.

RESULTS AND DISCUSSION

Synthesis of Octadentate Ligand 3,4,3-LI(CAM). Since electrostatic interactions between Scn and Ln/An complexes play a key role in binding, we chose to explore ligands that would form overall negative complexes with both 3+ and 4+ metals. Although Scn exhibits a broad, degenerate recognition mechanism for native siderophores, previous studies probing the extent of Scn binding to synthetic siderophore analogues showed that the Scn binding site allows only limited changes to its ligands.[21,26] Thus, the simplest way to correct the binding would be to employ ligands with similar structural features. We chose to follow Occam's razor by using 3,4,3-LI(CAM) (Figure 1), a compound first prepared by Raymond and co-workers for plutonium decorporation purposes.[27] This octadentate ligand leverages grafting of catecholamide (CAM) moieties found in microbial siderophores on the spermine scaffold to form a hybrid version of Ent and 3,4,3-LI(1,2-HOPO) that should (i) display increased complex stability over Ent due to its higher denticity and (ii) bear more negative charges than 3,4,3-LI(1,2-HOPO) due to CAM units requiring further deprotonation for metal binding (Figure 1). 3,4,3-LI(CAM) was synthesized here from readily available building blocks using a process developed in-house (Scheme 1). The new preparation moves away from

Scheme 1. Synthesis of 3,4,3-LI(CAM).[a]

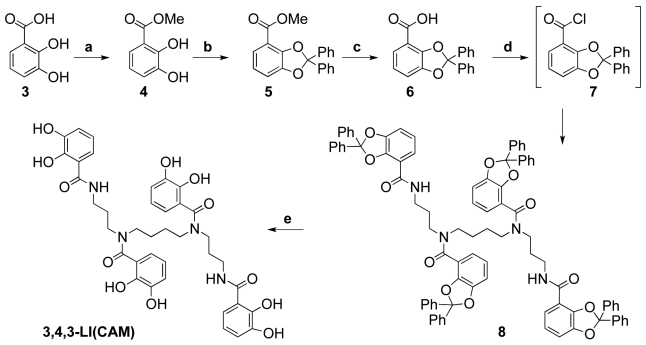

[a](a) H_2SO_4, MeOH, 65°C, 16 h (88%). (b) Dichlorodiphenylmethane, 160°C, 1 h. (c) 50/50 THF/H_2O, reflux 5 h (81% over 2 steps). (d) $(COCl)_2$, toluene, cat. DMF; then spermine, Et_3N, THF, 50°C, O/N (78%). (e) AcOH/H_2O + conc HCl, 16 h (90%).

using harsh reaction conditions by using the protected diphenylmethylene acetal derivative (**5**), which greatly simplifies purification of the final product.

Affinity of 3,4,3-LI(CAM) toward 3+ and 4+ Metals. A comprehensive solution thermodynamic analysis was performed to characterize the affinity of 3,4,3-LI(CAM) for trivalent and tetravalent metals and to understand the effect of substituting 1,2-HOPO for CAM binding units on the octadentate spermine scaffold. The protonation constants of 3,4,3-LI(CAM) were determined by spectrophotometric titrations, and eight protonation equilibria were assigned to sequential removal of two protons from each of the four CAM units (Table 1). Previous studies of Ent and other CAM-containing synthetic analogues established that the protonation constants (pK_{a1}−pK_{a4}) of the meta-hydroxyl oxygen atoms are well-separated from the ortho-hydroxyl oxygen atoms (pK_{a5}−pK_{a8}).[28] The last four pK_a values are most relevant to metal binding as moieties corresponding to these values have to be deprotonated at physiological pH in order to bind the metal ions. The overall acidity of 3,4,3-LI(CAM) can be defined as $\sum pK_{a5-8}$ = 27.8 versus 3,4,3-LI(1,2-HOPO)'s 21.2,[29] with lower values representing higher acidity. 3,4,3-LI(CAM) is therefore less prone to bind hard Lewis acids at low pH than its 1,2-HOPO analogue, due to competition between metal uptake and protonation of the CAM moieties.

Incremental spectrophotometric titrations were then carried out to determine the formation of Eu^{III}, Zr^{IV}, or Th^{IV} complexes with 3,4,3-LI(CAM). Because of the relatively short half-life of ^{225}Ac and the scarce availability of the longer-lived ^{227}Ac, Eu^{III} was used here as a nonradioactive Ln surrogate for Ac^{III}. On the basis of previous solution thermodynamic studies of Ln^{III} complexes of 3,4,3-LI(1,2-HOPO) and other common polyaminocarboxylate ligands,[24] it is reasonable to expect similar stability constants for Eu^{III} and Ac^{III} complexes of 3,4,3-LI(CAM). The 3,4,3-LI(CAM) octadentate ligand showed a very high affinity for both 3+ and 4+ ions (Table 1). The stability constants of $[Eu^{III}$-3,4,3-LI(CAM)$]^{5-}$, $[Th^{IV}$-3,4,3-LI(CAM)$]^{4-}$, and $[Zr^{IV}$-3,4,3-LI(CAM)$]^{4-}$ are several orders of magnitude higher than those of their 1,2-HOPO counter-

DOI: 10.1021/acs.inorgchem.6b02041
Inorg. Chem. XXXX, XXX, XXX−XXX

Table 1. Protonation and Eu^{III}, Zr^{IV}, and Th^{IV} Complex Formation Constants for 3,4,3-LI(CAM)[a]

species	*mlh*	log β_{mlh}	pK_a
		3,4,3-LI(CAM)	
LH^{7-}	011	12.50 ± 0.30	12.50 ± 0.30
LH_2^{6-}	012	24.50 ± 0.35	12.00 ± 0.30
LH_3^{5-}	013	35.81 ± 0.55	11.31 ± 0.55
LH_4^{4-}	014	45.41 ± 0.47	9.60 ± 0.12
LH_5^{3-}	015	54.11 ± 0.23	8.70 ± 0.27
LH_6^{2-}	016	61.93 ± 0.56	7.82 ± 0.57
LH_7^{-}	017	68.67 ± 1.45	6.73 ± 0.61
LH_8	018	73.24 ± 1.38	4.57 ± 0.29
$[EuL]^{5-}$	110	29.65 ± 0.65	
$[EuLH]^{4-}$	111	41.75 ± 0.06	
$[EuLH_2]^{3-}$	112	46.79 ± 0.14	
$[ZrL]^{4-}$	110	57.26 ± 0.20	
$[ZrLH]^{3-}$	111	64.25 ± 0.32	
$[ThL]^{4-}$	110	47.71 ± 0.08	
$[ThLH]^{3-}$	111	55.36 ± 0.09	
		3,4,3-LI(1,2-HOPO)	
LH^{3-}	011	6.64	6.64
LH_2^{2-}	012	12.32	5.68
LH_3^{-}	013	17.33	5.01
LH_4	014	21.20	3.87
$[EuL]^{-}$	110	20.2	
[EuLH]	111	24.8	
[ZrL]	110	43.1	
[ThL]	110	40.1	

[a] I = 0.1 M (KCl), T = 25 °C. Errors correspond to standard deviations from at least three independent titrations. Protonation and Eu^{III},[6] Zr^{IV},[7] and Th^{IV}[8] complex formation constants previously reported for 3,4,3-LI(1,2-HOPO) are also given for comparison.

parts, with log β_{110} values of 29.7, 47.7, and 57.3, respectively. Consequently, 3,4,3-LI(CAM) is one of the strongest ligands ever reported for the chelation of both trivalent and tetravalent f-elements. For comparison, a cyclic octadentate terephthalamide derivative was recently designed to bind Th^{4+} *in vivo* and showed an unprecedented affinity for Th^{4+} with a log β_{110} (ThL^{4-}) value of 53.7.[30] It is worth mentioning, however, that terephthalamide ligands would not be recognized by Scn, due to steric hindrance generated by the bulky substituents on the *para* position of the catecholate-like unit. To inspect the pH dependency of metal complex formation, speciation diagrams were calculated for 3,4,3-LI(CAM) in the presence of 1 equivalent of Eu^{III}, Zr^{IV}, or Th^{IV} (Figures S1–S3). Both Zr^{IV} and Th^{IV} complexes start forming at around pH 3, with the mono and fully deprotonated species, $[M^{IV}LH]^{3-}$ and $[M^{IV}L]^{4-}$, being predominant at physiological pH (7.4). This behavior departs from that of 3,4,3-LI(1,2-HOPO), with which 4^+ metal complexes are formed even under very acidic conditions (pH < 0).[31,32] For Eu^{III}, complexation by 3,4,3-LI(CAM) starts at pH 5, and the monoprotonated complex, $[Eu^{III}LH]^{4-}$, is the only species present at pH 7.4. Similar to what is observed with 4^+ metals, the pH at which Eu^{III}-3,4,3-LI(CAM) complexes start forming is higher than in the case of Eu^{III}-3,4,3-LI(1,2-HOPO) species that already appear at pH ∼ 1 under those same conditions.[29] However, it is important to note the multiple negative charges of the 3,4,3-LI(CAM) complexes with 3^+ and 4^+ metal complexes under physiologically relevant conditions ($[M^{III}LH]^{4-}$, $[M^{IV}LH]^{3-}$, and $[M^{IV}L]^{4-}$), which are now capable of forming electrostatic interactions with the Scn protein. This represents a large advantage over 3,4,3-LI(1,2-HOPO), for which the complexes with M^{III} at pH 7.4 have only one negative charge and are neutral in the case of M^{IV} ions.

Scn Recognition of 3,4,3-LI(CAM)-Metal Complexes. As described in several previous reports,[15,21,33] the affinity of Scn for ligands or metal–ligand complexes is quantified by monitoring protein fluorescence quenching upon ligand or complex binding. The equilibrium dissociation constant of Scn for the apo form of the ligand 3,4,3-LI(CAM), K_d = 1.2 ± 0.4 nM, is nearly identical to that determined for the native siderophore apo-Ent,[21] indicating that the addition of a fourth CAM unit does not affect ligand recognition by the protein. Subsequent determination of K_d values for various metal complexes of 3,4,3-LI(CAM) (M^{III} = Sm, Eu, Gd, ^{243}Am, or ^{248}Cm, and M^{IV} = Zr, ^{232}Th, or ^{242}Pu) confirms tight binding to the protein, independent of the metal valence, with values well below 40 nM (Figure 2). As hypothesized, these data

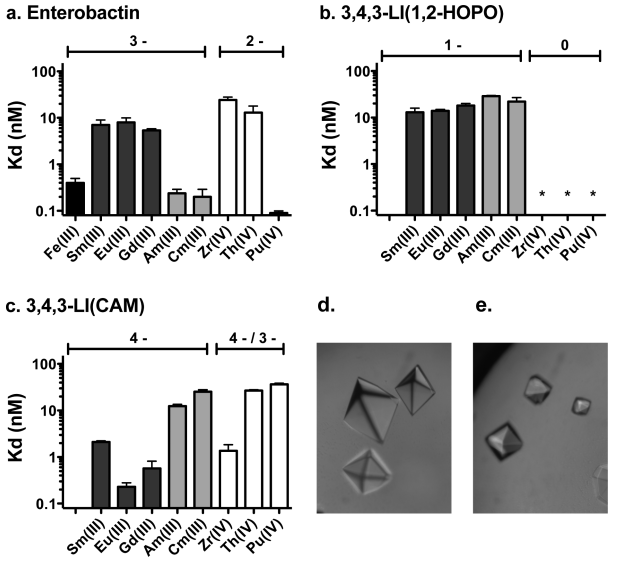

Figure 2. Scn dissociation constants determined from fluorescence quenching analyses for M^{III} and M^{IV} complexes formed with Ent[15] (a, top left), 3,4,3-LI(1,2-HOPO)[15] (b, top right), or 3,4,3-LI(CAM) (c, bottom left), and crystal pictures for the Scn adducts formed with the Zr^{IV} (d, bottom middle) and Th^{IV} (e, bottom right) complexes of 3,4,3-LI(CAM). The charges of the discussed metal complexes vary from 0 to 4− at pH 7.4 and are indicated above each bar; asterisks indicate that no binding was observed. Ent and 3,4,3-LI(1,2-HOPO) data are plotted on the basis of previously reported values,[15] except for the Zr complex K_d values that were determined in this work; the affinity observed with the ferric complex of Ent is shown for reference, as it is the native Scn ligand.

demonstrate a substantial difference in protein recognition between the 3,4,3-LI(CAM) and 3,4,3-LI(1,2-HOPO) complexes of tetravalent metals. Use of the diprotic CAM units in lieu of the monoprotic 1,2-HOPO moieties led to the formation of negatively charged complexes, enabling electrostatic interactions with the protein trilobal calyx. Moreover, while the addition of a fourth CAM metal-binding group in the octadentate 3,4,3-LI(CAM) was important for increased stability of the metal–ligand complexes at pH 7.4, it did not prevent the high Scn affinities initially observed with hexacoordinated Ent complexes. Subtle differences were observed with the recognition patterns: for similarly charged

DOI: 10.1021/acs.inorgchem.6b02041
Inorg. Chem. XXXX, XXX, XXX–XXX

complexes, weaker binding was observed with actinide complexes (Am^{III}, Cm^{III}, Th^{IV}, and Pu^{IV}) as compared to corresponding lanthanide or d-block metal complexes (Sm^{III}, Eu^{III}, Gd^{III}, Zr^{IV}) in the case of 3,4,3-LI(CAM). The opposite trend had been noted with Ent complexes of M^{III} metals[15] and was confirmed here with Zr^{IV}, while no significant differences are discernible with 3,4,3-LI(1,2-HOPO).

Structural Characterization of Scn-3,4,3-LI(CAM) Adducts. X-ray crystallography was used as previously described[15] to determine the structures of the Scn adducts formed with the ^{232}Th-3,4,3-LI(CAM) and Zr-3,4,3-LI(CAM) complexes (Table S1). As expected, and as observed in previous Scn complex structures (e.g., with ^{243}Am-3,4,3-LI(1,2-HOPO)),[15] the compounds are bound in the deeply recessed trilobal binding site, or calyx, of Scn (Figure 3a–c). As in previous structures of Scn bound to CAM-bearing ligands with An ions, only one CAM substituent is ordered in the crystal structures along with the bound metal, Zr or Th. This was likely a result of the remainder of the chelator sampling multiple conformations between molecules in the crystal, but clearly confirmed binding of chelator and metal in both adducts. The CAM substituent bound in the key binding pocket in the Scn calyx, between the side-chains of two bracketing lysine residues (K125 and K134; Figure 3d). The structure of the Scn calyx is highly conserved with prior structures, reflecting its rigidity, with the side-chains of two residues, W79 and R81, as the only elements flexing to accommodate different ligands (Figure 3e). In prior Ent or Ent analogue chelator/actinide structures,[15] where two of the three CAM groups are also disordered, the side-chain of W79 adopted an unusual rotamer, flipping inward toward the metal to contribute a cation–π interaction. However, in these structures, this side-chain adopts more conventional orientations, either sampling multiple rotamers, rendering it disordered in the crystallographic analysis (in the Zr complex), or lying against the calyx wall in the Th complex. Apart from these two side-chains, the overall impression conveyed by these and previous results is that the chelator flexes and distorts to fit in an essentially rigid and unyielding calyx.

Biodistribution Evaluation of Scn-3,4,3-LI(CAM) Adducts. To evaluate the *in vivo* retention and excretion patterns of M^{IV}-3,4,3-LI(CAM) complexes and their Scn adducts, $^{238}Pu^{IV}$ was used as a radiolabel. ^{238}Pu was selected as a surrogate radiometal to mimic ^{227}Th or ^{89}Zr for the following reasons: (i) It forms tetravalent coordination species under physiological conditions. (ii) Its ionic radius is between those of Zr^{IV} and Th^{IV}.[32] (iii) It is easier to handle and allows for more accurate metabolic balance experiments due to its relatively long radioactive half-life (87.8 years) and low specific activity (0.63 TBq/g), compared to the therapeutic ^{227}Th (18.7 d; 1139 TBq/g) and imaging ^{89}Zr (78.4 h; 16,630 TBq/g) isotopes. (iv) Natural Zr or other commonly available isotopes such as ^{232}Th (14 Gyr; 4.07 kBq/g) would not exhibit enough activity to allow for radioanalysis. In this *in vivo* stability experiment, ^{238}Pu–ligand complex solutions were formed *in situ* (ligand:Pu and Scn:ligand:Pu ratios of 100:1 and 100:100:1, respectively) and administered intravenously. Mice were euthanized 4, 24, or 48 h after the metal injection, and tissues and excreta were radioanalyzed for ^{238}Pu content (Figure 4). Independent of the presence of Scn in the administered solution, about 30% of the injected ^{238}Pu was excreted by 48 h, and ^{238}Pu excreta content steadily increased, suggesting delayed clearance of the complexes. The rate of ^{238}Pu elimination observed for ^{238}Pu-3,4,3-LI(CAM) is strikingly different from that observed for the ^{238}Pu-3,4,3-LI(1,2-HOPO) complex in previous studies (albeit performed in a different strain of mice and with younger animals), in which quantitative excretion was observed by 24 h. In both Scn-bound and free ^{238}Pu-3,4,3-LI(CAM) cases, and at all time points, more ^{238}Pu was found in the urine than in the feces. However, the kidney and liver contents reveal a key difference in excretion pattern: when free, the 3,4,3-LI(CAM) complex is predominantly found in the liver at early time points after administration and follows a biliary pathway, similar to what is known for HOPO complexes. However, insertion within the protein favors elimination through the renal system, with up to ~52% of ^{238}Pu found in the kidneys 4 h after administration of the Scn adducts, a burden that subsequently

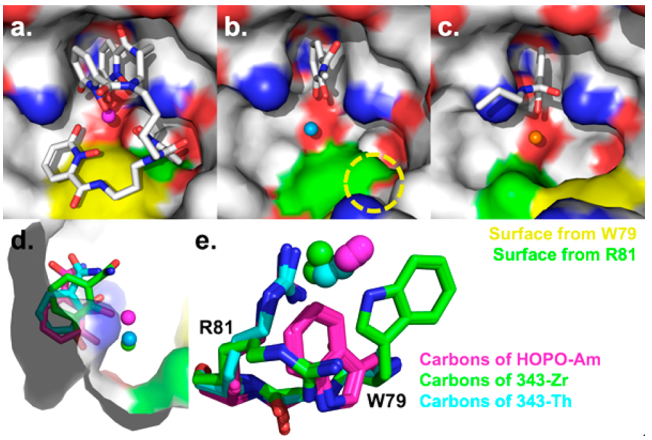

Figure 3. Crystallographic analyses of the binding of ^{232}Th-3,4,3-LI(CAM) and Zr-3,4,3-LI(CAM) by Scn. (a) A molecular surface representation of the calyx of Scn is colored by atom type (C, gray; O, red; N, blue), with the ^{243}Am-3,4,3-LI(1,2-HOPO) complex[15] shown in a licorice-stick representation, also colored by atom type. The metal ion is shown as a small sphere, colored magenta. Surfaces contributed by the side-chains of W79 and R81 are colored yellow and green, respectively. Two prominent blue-tipped protuberances sticking into the calyx correspond to the side-chains of K125 and K134, which bracket the crucial binding pocket in the calyx. (b) A view into the Scn calyx of the ^{232}Th-3,4,3-LI(CAM) complex structure, shown as in part a. In this structure, the side-chain of W79 is disordered, indicated by the yellow dashed circle, due to sampling of multiple rotamers in the complex, allowing much more of the surface of R81 to be seen. Only one substituent CAM group and the actinide (aqua sphere) are ordered and visualized in the complex crystal structure, as had been seen in a previous hexadentate CAM/actinide/Scn structure.[15] The one ordered CAM moiety sits in the key binding pocket defined by the side-chains of K125 and K134. (c) A view into the Scn calyx of the Zr-3,4,3-LI(CAM) complex structure, shown as in parts a and b. In this structure, the side-chains of W79 and R81 have repositioned to accommodate this ligand. Like the ^{232}Th structure, only one substituent CAM group and the Zr atom (orange sphere) are ordered. (d) A view perpendicular to that in parts a–c highlights the differential packing of the CAM or HOPO substituents in the key binding pocket. Other atoms in the chelator have been removed for clarity, and the molecular surface has been rendered partially transparent. Metal and carbon atoms have been recolored to indicate the complex: ^{243}Am-3,4,3-LI(1,2-HOPO) in magenta, ^{232}Th-3,4,3-LI(CAM) in aqua, and Zr-3,4,3-LI(CAM) in green. (e) The side-chains of W79 and R81 and the connecting protein backbone have been isolated and superimposed from the three complexes; they are shown in a licorice-stick representation, colored as in part d. This view highlights the different rotamers selected in the different complexes, the only element of conformational flexibility in the extremely rigid Scn calyx.[15]

DOI: 10.1021/acs.inorgchem.6b02041
Inorg. Chem. XXXX, XXX, XXX–XXX

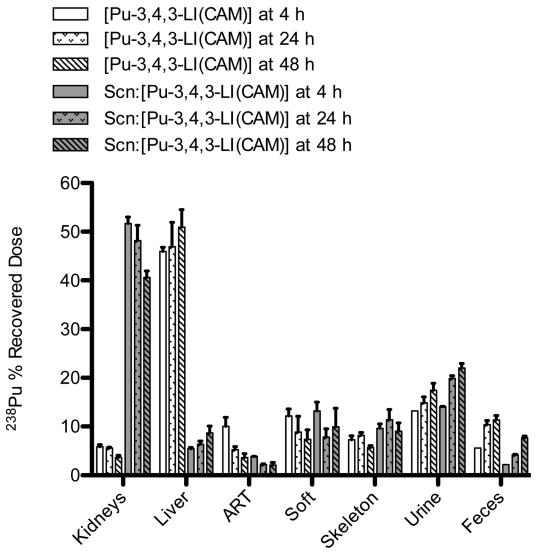

Figure 4. Biodistribution of Pu^{IV} when administered as a free or Scn-bound 3,4,3-LI(CAM) complex. Healthy mice injected intravenously with ^{238}Pu–ligand and ^{238}Pu–ligand–protein solutions (370 Bq/mouse); mice euthanized at 4, 24, or 48 h. "ART" and "Soft" stand for "abdominal remaining tissues" and other "soft tissues", respectively.

slowly decreases. In combination with significantly faster rates of excretion and considerably lower skeleton and soft tissue burden when compared with free ^{238}Pu, this major difference between kidney versus liver ^{238}Pu retention of the Scn-bound versus free complex provide evidence for the high *in vivo* stability of the Scn:[Pu^{IV}(3,43-LI(CAM))] adduct.

CONCLUSIONS

Results obtained with the Scn:3,4,3-LI(CAM) system suggest a novel concept that enables the engineering of new radiopharmaceuticals comprising protein targeting vectors, such as antibodies, coupled with radionuclide capture moieties based on Scn. The protein's highly specific binding to 3,4,3-LI(CAM)-M^{IV} and 3,4,3-LI(CAM)-M^{III} complexes eliminates the need for costly synthetic bioconjugation of ligands to targeting molecules. Interestingly, one can envision a system where both imaging ($^{89}Zr^{IV}$) and therapeutic ($^{227}Th^{IV}$ or $^{225}Ac^{III}$) metallic radioisotopes may be used in conjunction for dual diagnostics/treatment applications. Our results illustrate the promise of this system. It is also likely that, with further tuning, a more effective protein–ligand arrangement may be developed: current work is underway to explore other ligands based on the 3,4,3-LI scaffold in order to reconcile the metal/protein binding compromise by incorporating both monoprotic HOPO and diprotic CAM units. Finally, future efforts will focus on evaluating the kinetics of release of different radionuclides from the Scn:ligand systems, as well as the distribution of daughter products. We will perform *in vitro* and *in vivo* studies with the more suited medical isotopes ^{225}Ac, ^{227}Th, and ^{89}Zr, in lieu of the low-activity surrogates used in the presented solution studies.

ASSOCIATED CONTENT

Supporting Information

The Supporting Information is available free of charge on the ACS Publications website at DOI: 10.1021/acs.inorgchem.6b02041.

Detailed experimental procedures; NMR and mass spectra of protected and deprotected 3,4,3-LI(CAM); examples of spectrophotometric titrations and speciation diagrams for the scavenging of Eu^{III}, Zr^{IV}, and Th^{IV} by 3,4,3-LI(CAM); and crystallographic statistics for Scn:3,4,3-LI(CAM) bound to Zr^{IV} and Th^{IV} (PDF)

AUTHOR INFORMATION

Corresponding Authors

*E-mail: rstrong@fhcrc.org.

*E-mail: rjabergel@lbl.gov.

Notes

The authors declare no competing financial interest.

ACKNOWLEDGMENTS

This material is based upon work supported by the U.S. Department of Energy, Office of Science, Office of Basic Energy Sciences, Chemical Sciences, Geosciences, and Biosciences Division at the Lawrence Berkeley National Laboratory under Contract DE-AC02-05CH11231 (R.J.A.), and by the National Institutes of Health under award number R01DK073462 (subcontract to R.K.S.). R.J.A. is the recipient of a U.S. Department of Energy, Office of Science Early Career Award. M.-C.I. is the recipient of a mobility grant from the ParisTech chair of nuclear engineering supported by Areva. The Advanced Light Source (ALS) is supported by the Director, Office of Science, Office of Basic Energy Sciences, of the U.S. Department of Energy under Contract DE-AC02-05CH11231. We thank M. Allaire, S. Morton, J. Bramble, K. Engle, I. Tadesse, and M. Dupray for their assistance in planning and implementing diffraction data collection on radioactive crystals at the ALS 5.0.2 beamline. We also thank K. Raymond for providing us with purified Ent. The content is solely the responsibility of the authors and does not necessarily represent the official views of the National Institutes of Health.

REFERENCES

(1) Mulford, D. A.; Scheinberg, D. A.; Jurcic, J. G. The promise of targeted α-particle therapy. *J. Nucl. Med.* **2005**, *46*, 199S–204S.

(2) Kim, Y. S.; Brechbiel, M. W. *Tumor Biol.* **2012**, *33*, 573–590.

(3) McDevitt, M. R.; Ma, D.; Lai, L. T.; Simon, J.; Borchardt, P.; Frank, R. K.; Wu, K.; Pellegrini, V.; Curcio, M. J.; Miederer, M.; Bander, N. H.; Scheinberg, D. A. Tumor Therapy with Targeted Atomic Nanogenerators. *Science* **2001**, *294*, 1537–1540.

(4) Aghevlian, S.; Boyle, A. J.; Reilly, R. M. Radioimmunotherapy of cancer with high linear energy transfer (LET) radiation delivered by radionuclides emitting α-particles or Auger electrons. *Adv. Drug Delivery Rev.* **2015**, DOI: 10.1016/j.addr.2015.12.003.

(5) Knapp, F. F.; Dash, A. Alpha Radionuclide Therapy. In *Radiopharmaceuticals for Therapy*; Springer India: New Delhi, 2016; pp 37–55.

(6) Read, E. D.; Eu, P.; Little, P. J.; Piva, T. J. The status of radioimmunotherapy in CD20+ non-Hodgkin's lymphoma. *Targeted Oncology* **2015**, *10*, 15–26.

(7) Liepe, K. Alpharadin, a 223Ra-based alpha-particle-emitting pharmaceutical for the treatment of bone metastases in patients with cancer. *Current opinion in investigational drugs (London, England: 2000)* **2009**, *10*, 1346–1358.

(8) Ravandi, F.; Pagel, J. M.; Park, J. H.; Douer, D.; Estey, E. H.; Kantarjian, H. M.; Cicic, D.; Scheinberg, D. A. Phase I trial of the targeted alpha-particle nano-generator actinium-225 (225Ac)-lintuzumab (anti-CD33) in combination with low-dose cytarabine (LDAC) for older patients with untreated acute myeloid leukemia (AML). *Blood* **2013**, *122*, 1460–1460.

DOI: 10.1021/acs.inorgchem.6b02041
Inorg. Chem. XXXX, XXX, XXX–XXX

(9) Hagemann, U. B.; Wickstroem, K.; Wang, E.; Shea, A. O.; Sponheim, K.; Karlsson, J.; Bjerke, R. M.; Ryan, O. B.; Cuthbertson, A. S. In vitro and in vivo efficacy of a novel CD33 targeted thorium-227 conjugate for the treatment of acute myeloid leukemia. *Mol. Cancer Ther.* **2016**, *15*, 2422.
(10) Heyerdahl, H.; Abbas, N.; Brevik, E. M.; Mollatt, C.; Dahle, J. Fractionated therapy of HER2-expressing breast and ovarian cancer xenografts in mice with targeted alpha emitting 227 Th-DOTA-p-benzyl-trastuzumab. *PLoS One* **2012**, *7*, e42345.
(11) Bunin, D. I.; Chang, P. Y.; Doppalapudi, R. S.; Riccio, E. S.; An, D. D.; Jarvis, E. E.; Kullgren, B.; Abergel, R. J. Efficacy and Safety Toxicology of Hydroxypyridinonate Actinide Decorporation Agents in Rodents: Towards a Safe and Effective Human Dosing Regimen. *Radiat. Res.* **2013**, *179*, 171−182.
(12) Deri, M. A.; Ponnala, S.; Kozlowski, P.; Burton-Pye, B. P.; Cicek, H. T.; Hu, C.; Lewis, J. S.; Francesconi, L. C. p-SCN-Bn-HOPO: A Superior Bifunctional Chelator for 89Zr ImmunoPET. *Bioconjugate Chem.* **2015**, *26*, 2579−2591.
(13) Deri, M. A.; Ponnala, S.; Zeglis, B. M.; Pohl, G.; Dannenberg, J. J.; Lewis, J. S.; Francesconi, L. C. Alternative Chelator for Zr-89 Radiopharmaceuticals: Radiolabeling and Evaluation of 3,4,3-(LI-1,2-HOPO). *J. Med. Chem.* **2014**, *57*, 4849−4860.
(14) Ramdahl, T.; Bonge-Hansen, H. T.; Ryan, O. B.; Larsen, Å.; Herstad, G.; Sandberg, M.; Bjerke, R. M.; Grant, D.; Brevik, E. M.; Cuthbertson, A. S. An efficient chelator for complexation of thorium-227. *Bioorg. Med. Chem. Lett.* **2016**, *26*, 4318−4321.
(15) Allred, B. E.; Rupert, P. B.; Gauny, S. S.; An, D. D.; Ralston, C. Y.; Sturzbecher-Hoehne, M.; Strong, R. K.; Abergel, R. J. Siderocalin-mediated recognition, sensitization, and cellular uptake of actinides. *Proc. Natl. Acad. Sci. U. S. A.* **2015**, *112*, 10342−10347.
(16) Clifton, M. C.; Corrent, C.; Strong, R. K. Siderocalins: siderophore-binding proteins of the innate immune system. *BioMetals* **2009**, *22*, 557−564.
(17) Gorden, A. E.; Shuh, D. K.; Tiedemann, B. E.; Wilson, R. E.; Xu, J.; Raymond, K. N. Sequestered Plutonium:$[Pu^{IV}\{5LIO(Me\text{-}3, 2\text{-}HOPO)\}_2]^-$The First Structurally Characterized Plutonium Hydroxypyridonate Complex. *Chem. - Eur. J.* **2005**, *11*, 2842−2848.
(18) Welcher, F. J. *Analytical Uses of Ethylenediamine Tetraacetic Acid*; D. Van Nostrand Co., 1958
(19) Goetz, D. H.; Holmes, M. A.; Borregaard, N.; Bluhm, M. E.; Raymond, K. N.; Strong, R. K. The neutrophil lipocalin NGAL is a bacteriostatic agent that interferes with siderophore-mediated iron acquisition. *Mol. Cell* **2002**, *10*, 1033−1043.
(20) Sturzbecher-Hoehne, M.; Deblonde, G.-P.; Abergel, R. Solution thermodynamic evaluation of hydroxypyridinonate chelators 3, 4, 3-LI (1, 2-HOPO) and 5-LIO (Me-3, 2-HOPO) for UO2 (VI) and Th (IV) decorporation. *Radiochim. Acta* **2013**, *101*, 359−366.
(21) Abergel, R. J.; Moore, E. G.; Strong, R. K.; Raymond, K. N. Microbial evasion of the immune system: structural modifications of enterobactin impair siderocalin recognition 1. *J. Am. Chem. Soc.* **2006**, *128*, 10998−10999.
(22) Berman, H. M.; Westbrook, J.; Feng, Z.; Gilliland, G.; Bhat, T. N.; Weissig, H.; Shindyalov, I. N.; Bourne, P. E. The Protein Data Bank. *Nucleic Acids Res.* **2000**, *28*, 235−242.
(23) Kullgren, B.; Jarvis, E. E.; An, D. D.; Abergel, R. J. Actinide chelation: biodistribution and in vivo complex stability of the targeted metal ions. *Toxicol. Mech. Methods* **2013**, *23*, 18−26.
(24) Sturzbecher-Hoehne, M.; Leung, C. N. P.; D'Aléo, A.; Kullgren, B.; Prigent, A.-L.; Shuh, D. K.; Raymond, K. N.; Abergel, R. J. 3, 4, 3-LI (1, 2-HOPO): In vitro formation of highly stable lanthanide complexes translates into efficacious in vivo europium decorporation. *Dalton Trans.* **2011**, *40*, 8340−8346.
(25) Durbin, P. W.; Kullgren, B.; Ebbe, S. N.; Xu, J.; Raymond, K. N. Chelating agents for uranium (VI): 2. Efficacy and toxicity of tetradentate catecholate and hydroxypyridinonate ligands in mice. *Health Phys.* **2000**, *78*, 511−521.
(26) Holmes, M. A.; Paulsene, W.; Jide, X.; Ratledge, C.; Strong, R. K. Siderocalin (Lcn 2) also binds carboxymycobactins, potentially defending against mycobacterial infections through iron sequestration. *Structure* **2005**, *13*, 29−41.
(27) Weitl, F. L.; Raymond, K. N. Specific sequestering agents for the actinides. 3. Polycatecholate ligands derived from 2, 3-dihydroxy-5-sulfobenzoyl conjugates of diaza-and tetraazaalkanes. *J. Am. Chem. Soc.* **1980**, *102*, 2289−2293.
(28) Loomis, L. D.; Raymond, K. N. Solution equilibria of enterobactin and metal-enterobactin complexes. *Inorg. Chem.* **1991**, *30*, 906−911.
(29) Abergel, R. J.; D'Aléo, A.; Ng Pak Leung, C.; Shuh, D. K.; Raymond, K. N. Using the Antenna Effect as a Spectroscopic Tool: Photophysics and Solution Thermodynamics of the Model Luminescent Hydroxypyridonate Complex $[Eu^{III}(3, 4, 3\text{-}LI (1, 2\text{-}HOPO))]^-$. *Inorg. Chem.* **2009**, *48*, 10868−10870.
(30) Pham, T. A.; Xu, J.; Raymond, K. N. A Macrocyclic Chelator with Unprecedented Th^{4+} Affinity. *J. Am. Chem. Soc.* **2014**, *136*, 9106−9115.
(31) Deblonde, G. J.; Sturzbecher-Hoehne, M.; Abergel, R. J. Solution thermodynamic stability of complexes formed with the octadentate hydroxypyridinonate ligand 3, 4, 3-LI (1, 2-HOPO): a critical feature for efficient chelation of lanthanide (IV) and actinide (IV) ions. *Inorg. Chem.* **2013**, *52*, 8805−8811.
(32) Sturzbecher-Hoehne, M.; Choi, T. A.; Abergel, R. J. Hydroxypyridinonate complex stability of group (IV) metals and tetravalent f-block elements: The key to the next generation of chelating agents for radiopharmaceuticals. *Inorg. Chem.* **2015**, *54*, 3462−3468.
(33) Abergel, R. J.; Wilson, M. K.; Arceneaux, J. E.; Hoette, T. M.; Strong, R. K.; Byers, B. R.; Raymond, K. N. Anthrax pathogen evades the mammalian immune system through stealth siderophore production. *Proc. Natl. Acad. Sci. U. S. A.* **2006**, *103*, 18499−18503.

DOI: 10.1021/acs.inorgchem.6b02041
Inorg. Chem. XXXX, XXX, XXX−XXX